Freeze drying and rehydration of alginate fluid gels

Smaniotto, Fabio; Prosapio, Valentina; Zafeiri, Ioanna; Spyropoulos, Fotios

DOI:
10.1016/j.foodhyd.2019.105352

Document Version
Peer reviewed version

Citation for published version (Harvard):
Smaniotto, F, Prosapio, V, Zafeiri, I & Spyropoulos, F 2020, 'Freeze drying and rehydration of alginate fluid gels', *Food Hydrocolloids*, vol. 99, 105352. https://doi.org/10.1016/j.foodhyd.2019.105352

Freeze drying and rehydration of alginate fluid gels

F. Smaniotto, V. Prosapio*, I. Zafeiri, F. Spyropoulos

School of Chemical Engineering, University of Birmingham, Edgbaston, Birmingham B15 2TT, United Kingdom

*v.prosapio@bham.ac.uk

Abstract

The aim of this work was to study the effect of freeze drying (FD) and rehydration on alginate fluid gels (AFG). FD was employed as a widely used drying method in order to evaluate whether its application causes any change in the material characteristics crucial for AFG behaviour. Rehydration studies were performed to assess if AFG properties could be restored after drying and rehydration processes. First, it was investigated the influence of the material formulation (alginate (ALG) and calcium chloride ($CaCl_2$) concentrations) on the particle size distribution (PSD) and the rheological properties. The used ALG/$CaCl_2$ ratio demonstrated to be responsible for forming nanoparticles or microparticles. The impact of fluid gel particle dimensions on drying and rehydration processes was also investigated. Overall, particle dimensions do not have a significant effect on drying kinetics. Analyses on rehydrated samples showed that the PSD is not affected by the processing, whereas the same viscosity was completely recovered only for samples formed by ALG and $CaCl_2$ in quantities leading to nanoparticles formation. Preliminary encapsulation experiments were also carried out to highlight the impact of this process on the release behaviour of the loaded active from AFG. Results obtained from in vitro release studies and their model fitting showed that the active release behaviour from AFG was not affected by freeze drying when AFG was formed of nanoparticles. On the contrary, the active release behaviour was affected by freeze drying when AFG was formed by microparticles.

Keywords: Fluid gel; freeze-drying; rehydration; rheological properties; encapsulation

1. Introduction

Fluid gels are suspensions of gel particles in a non-gelled continuous medium and are formed by applying shear forces to a polymeric solution undergoing a sol-gel transition (Garrec & Norton, 2012). They can be prepared using both biological (polysaccharides and proteins) and synthetic polymers (Norton, et al., 1999), and can be produced using typical shear devices, such as a jacketed pin-stirrer, which allows a continuous process. Fluid gels can be temperature and/or ionically set, depending on the hydrocolloid used and to its gelation mechanism (García, et al., 2018a; Wang, et al., 2016). The particle size can be controlled by varying the polymer concentration and the shear rate (García, et al., 2018b; Norton, et al., 1999).

Fluid gels show unique characteristics: at low deformations their flow behaviour tends to resemble that of quiescent gels, whereas at high deformations exhibits yield and flow characteristics like a viscoelastic fluid (Norton, et al., 2015). Due to this rheological performance, fluid gels find applications in the food industry as fat replacers (Chung, et al., 2014; Le Révérend, et al., 2010), texturing (Fernández Farrés, et al., 2014), satiety enhancers (Norton, et al., 2006) and emulsion stabiliser (García, et al., 2014). A novel application involves their use for encapsulation of bioactive molecules to protect them from the surrounding environment, to control their release in a specific medium and/or to mask their flavour (Mahdi, et al., 2016; Torres, et al., 2016). The use of fluid gels as encapsulating material has the following advantages compared to other carriers (such as microcapsules, liposomes, etc.): organic solvents are not needed, the process can be run in continuous and can be easily scaled-up, mild operating conditions can be employed and good control over particle size is provided.

Being formed by a large amount of water, the shelf-life of fluid gels is relatively short and microbial spoilage can easily occur. This limitation can be overcome by drying the material, as water removal prevents bacteria proliferation. A dried product can be considered as safe if it is characterised by water activity (a_w) lower than 0.6 (de Bruijn, et al., 2016) and normalised moisture content (NMC) lower than 0.1 (Brown, et al., 2010; Prosapio & Norton, 2018). In addition, the lower volume/weight of the product allows packaging, transport and storage costs to be reduced (Brown, et al., 2008; Prosapio, et al., 2017b). On the other hand, drying of food products has been reported to cause some damage to the product microstructure

according to the method and conditions employed, leading to low rehydration capacity and poor recovery of the initial properties (Vega-Gálvez, et al., 2015). Among the most common drying methods, freeze-drying (FD) showed the best performance in terms of water desorption, retention of the product characteristics and rehydration of the dried material (Karam, et al., 2016; Prosapio & Norton, 2017a). Specifically, for the dehydration of microstructures/formulations containing encapsulated matters, FD can be a suitable method to prevent the degradation of thermosensitive compounds, as it involves the freezing of the product, followed by ice sublimation under vacuum conditions (Barbosa, et al., 2015; Sanchez, et al., 2013).

The drying of quiescent gels has been extensively investigated using different materials (gellan gum (Bonifacio, et al., 2017; Cassanelli, et al., 2018), starch (De Marco & Reverchon, 2017; Franco, et al., 2018), cellulose (Jin, et al., 2004; Long, et al., 2018), agarose (Mao, et al., 2017), silica (Smirnova, et al., 2003), chitosan (Cardea, et al., 2010), etc.) and techniques (air-drying, freeze-drying, supercritical carbon dioxide drying, microwave drying (Cassanelli, et al., 2019; Hu, et al., 2013)). Tiwari et al. (Tiwari, et al., 2015) analysed the structure of freeze-dried gellan gum and agar gels; they observed for both materials that mechanically stable cellular solids were produced. Cassanelli et al. (Cassanelli, et al., 2019) studied the drying of gellan gum gels using oven drying, freeze drying and supercritical carbon dioxide drying; they observed that the gel microstructure was better preserved when FD was employed, leading to a significantly higher rehydration capacity compared to the other methods. Hu et al. (Hu, et al., 2013) employed air drying, microwave vacuum drying and freeze drying to dry hairtail fish meat gels and stated that FD samples showed better quality attributes in terms of moisture content, water absorption index, protein degradation and sensory acceptance than air and microwave-dried ones.

Despite the potentiality in providing long/safe storage and protection of the actives, the drying of fluid gels has not been studied so far. In order to fill the gap in the current literature, this work investigates the freeze drying of alginate fluid gels (AFG). Alginate is a hydrocolloid that undergoes gelation in the presence of multivalent cations, usually Ca^{2+} (McHugh & Pap, 1987). AFG were prepared in a pin-stirrer and thereafter freeze-dried. Rheological measurements were carried out on both unprocessed and processed fluid gels to verify if the material properties (particle size and viscosity) can be completely recovered after drying and

rehydration. In addition to the preservation of rheological behaviour upon rehydration, the capacity of the fluid gels to modulate the release of a model active (present within the fluid gel microstructure) prior and following FD was investigated. Preliminary encapsulation experiments were also performed, using Nicotinamide as model active, to investigate the release behaviour before and after drying/rehydration, and identify possible changes due to the processing.

2. Materials and methods

2.1 Materials

Sodium alginate (ALG), and nicotinamide (NIC, ≥98%, HPLC) were purchased from Sigma-Aldrich® (Sigma–Aldrich Company Ltd., Dorset, UK). Calcium chloride ($CaCl_2$, anhydrous, 93%) was purchased from Alfa Aesar™ (USA). All materials were used without further purification. Milli-Q water was made using an Elix® 5 distillation apparatus (Millipore®, USA) and was used for all water-based preparations.

2.2 Gel preparation

2.2.1 Blank fluid gels

Firstly, an alginate solution was prepared by dissolving different amounts of ALG (1%, 2%, 3% (w/w), calculated on the final weight of the material) in distilled water at 95°C for 45 min under stirring to ensure complete powder dissolution, as reported by Farrés et al. (Fernández Farrés, et al., 2013). Thereafter, the solution was cooled at room temperature (R.T.). Secondly, another solution was prepared by dissolving $CaCl_2$ at a different concentration for each experiment (0.15%, 0.25%, 0.35% (w/w), calculated on the final weight of the material) in water at R.T.. Alginate Fluid Gels (AFG) were prepared using a pin-stirrer vessel (Het Stempel, HL) having a volume of 150 mL, 16 pins placed on the rotating shaft and 16 pins fixed on the internal wall. 1000 rpm shaft speed was used for AFG production. The alginate solution was pumped using a flowrate of 33 mL/min with a peristaltic pump (Masterflex L/S Peristaltic, DE), while the $CaCl_2$ solution was injected using a flowrate of 4.02 mL/min with a syringe pump (Cole-Parmer Single-syringe, US) through a stainless steel needle of 1.25 mm internal diameter.

2.2.2 Nicotinamide fluid gels

Firstly, a solution of 2% (w/w) was prepared by dissolving ALG in distilled water at 95 °C for 45 min under stirring to ensure complete powder dissolution. Then, the solution was cooled at R.T.. Secondly, three solutions at 0.10% (w/w) were prepared by dissolving NIC in distilled water at R.T.. To these solutions different amounts of $CaCl_2$ (0.15%, 0.25%, 0.35% (w/w), calculated on the final weight) were dissolved at R.T.. Nicotinamide Fluid Gels (NFG) were then prepared using a pin-stirrer vessel as described above (2.2.1 Blank fluid gels).

2.3 Rheological properties

The rheological properties of fluid gels were determined by shear viscosity tests using a rotational rheometer (Kinexus™, Malvern®, UK) equipped with a 40 mm diameter sand blasted plate geometry. The analyses were carried out at 25 °C using a shear rate ramp of 31 points between 0.01 and 100 s^{-1}. Measurements were performed in triplicate.

2.4 Particle Size Distribution

2.4.1 Mastersizer

The particle size distribution (PSD) of fluid gels was evaluated using a Mastersizer-2000 (Malvern®, UK). Few drops of sample were placed into the mixing chamber and stirred for 10 min at 1300 rpm before performing the analysis to disrupt any possible macro-aggregation. PSD was evaluated as numerical particle sizes percentage. Measurements were performed in triplicate.

2.4.2 Zetasizer

The PSD of fluid gels was also evaluated by using Zetasizer (Malvern Instruments Ltd., UK). Samples were diluted with water before analysis to yield a suitable scattering intensity and measured at 25 °C. PSD curves were evaluated as numerical particle sizes percentage. All measurements were performed at 25 °C in triplicate.

2.5 Optical microscopy

Optical microscope (DM 2500 LED, Leica®, CH) was used to observe and record alginate microparticles. Samples were, firstly, diluted with distilled water using a water to sample ratio of 10:1 and they were mixed using a vortex mixer (VM20, Rigal Bennet®, UK) for 20 seconds. DIC settings were employed to increase the contrast, allowing the average dimensions of particles to be measured. Images were captured using a CCD camera (DFC450

C, Leica®, CH) coupled to the microscope. Image analysis software IPP (LAS 4.8.0, Leica®, CH) was used to evaluate the dimensions of the microparticles through the images.

2.6 Freeze drying

Fluid gels were frozen at -20 °C overnight and then lyophilised using a bench top Freeze Dryer (SCANVAC Coolsafe™, model 110-4, DK), condenser temperature -110 °C, pressure 10 Pa, condition that is defined by the equipment. The processing time was varied from 2 to 48 h to investigate the drying kinetics. Experiments were performed in triplicate for each condition investigated.

2.7 Moisture content analysis

Moisture content analyses were carried out measuring the sample weight before and after drying. Moisture content was expressed as NMC (Normalised Moisture Content) and calculated through the following equation (1):

$$NMC = \frac{(Md - Ms)}{(Mo - Ms)} \qquad (1)$$

where M_s is the solid sample mass, M_d the sample mass after drying and M_o the pre-dried sample. The drying kinetics was determined plotting NMC as a function of the drying time. Analyses were carried out in triplicate.

2.8 Water activity analysis

Water activity (a_w) of dried samples was measured using an AquaLab® dew point water activity meter (model 4TE, Decagon Devices Inc., Pullman, WA, USA). The temperature controlled sample chamber was set to 25 °C. Analyses were carried out in triplicate.

2.9 Rehydration of samples

After dehydration, amounts of distilled water were placed in each sample in order to obtain the same sample weight before FD. Samples were then transferred in a shacking incubator (Incu-Shake MIDI, SciQuip, UK), in order to obtain a homogeneous rehydration of the material, for different times at 400 rpm and 20 °C.

2.10 In vitro release

In vitro release studies from NFG were performed using a UV/vis spectrophotometer (Orion Aquamate, Thermo Scientific, UK) to determine the concentration of NIC in the medium over time. A weighted amount of NFG (approximatively 2.5 g) was enclosed in a dialysis sack (Sigma–Aldrich Company Ltd., Dorset, UK, dialysis tubing cellulose membrane, width 43 mm, M.W. cut-off of 14000 Da) and placed in 500 mL of distilled water at room temperature (thermostated at 21.5 ^{o}C), under stirring at 150 rpm. At regular intervals, aliquots of 2 mL were withdrawn, measured using the spectrophotometer at 214 nm wavelength and then poured again into the medium. A calibration curve was made at 214 nm wavelength (NIC maximum of absorbance) and was set for concentrations between 0.08 and 45 µg/mL and was used to correlate the absorbance value to the actual concentration of NIC into the release medium. Each analysis was carried out in triplicate.

2.11 Data fitting

Data obtained from NIC in vitro release studies from NFG were model fitted using equation (2):

$$\frac{M_t}{M_\infty} = kt^n \qquad (2)$$

where M_t and M_∞ are respectively the cumulative amounts of drug released at time t and at time when the release plateaux was reached, k is the kinetic constant and n is an exponent characterizing the diffusional mechanism. The use of Eq. (2) is validated by several authors and it is generally used to understand the release mechanism of drugs and bioactives from formulations from release data obtained in in vitro release experiments (Korsmeyer, et al., 1983; Rinaki, et al., 2003; Siepmann, et al., 2002).

3 Results and discussion

In the first part of the experimentation, the amounts of alginate (ALG) and $CaCl_2$ were varied to identify the minimum ratio between $CaCl_2$ and ALG required to obtain microparticles formation. Both formulations (forming and non-forming particles) were used as matrices for the encapsulation of nicotinamide. In vitro release behaviour of NIC from these materials was then studied. Freeze-drying experiments on AFG were carried out to investigate the effect of this method on fluid gel properties (particle size and viscosity) and to identify the conditions needed to assure the complete removal of free water (NMC < 0.1 and a_w < 0.6) (Brown, et al.,

2010; Ratti, 2001; Stevenson, et al., 2015). The effect of $CaCl_2$ concentration in AFG on the freeze drying kinetics was also investigated. Afterwards, a second set of release experiments was performed on NFG to study the effect of the freeze drying process and rehydration on the release behaviour of NIC from AFG.

3.1 Effect of ALG/$CaCl_2$ ratio

The amount of $CaCl_2$ needed to obtain the complete gelation of AFG was investigated by producing several samples at fixed ALG concentration and changing the $CaCl_2$ one; the final properties of the obtained materials in terms of PSD were then assessed. Samples compositions used in this part of the work alongside their acronyms are reported in Table 1.

3.1.1 Particle size distribution

Particle dimensions were evaluated using the Mastersizer and Zetasizer as reported in section 2.4 (Particle Size Distribution). PSD curves obtained using the Mastersizer and the Zetasizer are reported in Figure 1.

Mastersizer and Zetasizer curves of AFG_2%_0.35% displayed a PSD in the range of 0.5 to 5 µm, while AFG_2%_0.15% and AFG_2%_0.25% were in the range between 0.02 µm and 0.2 µm. The particle formation behaviour of samples was also studied using light microscopy (as shown in Figure 1b).

Due to the small dimensions, particles in samples AFG_2%_0.25% and AFG_2%_0.15% could not be recorded/visualised by optical microscopy analysis, while it can be noticed the presence of microparticles for AFG_2%_0.35% (Figure 1b). Samples were also produced using different percentages of ALG to identify the ratio between $CaCl_2$ and ALG necessary to ensure particle formation. Samples compositions used are reported in Table 2.

Microparticles formation was observed for samples AFG_1%_0.25% and AFG_3%_0.45%, while nanoparticles were detected for the samples AFG_1%_0.15% and AFG_3%_0.35%. These results showed that microparticles formation was achieved only when a critical ratio between ALG and $CaCl_2$ was used during sample preparation. This ratio can be estimated to be around 0.155 of $CaCl_2$ to ALG (w/w) and from now on this ratio will be called Critical Ratio for Microparticles Formation (CRMF). This value was estimated considering the used percentages of $CaCl_2$ and ALG in samples that consisted of microparticles. However, even

in samples produced with a $CaCl_2$/ALG ratio lower than the CRMF, PSD curves showed the presence of nanoparticles in the range of 100 nm and due to these very small dimensions they could not be visualised using optical microscopy.. In accordance with results reported by Badita et al., these nano-domains can be attributed to the alginate polymer chains morphology. Additionally, the authors observed the formation of an alginate secondary structure in the presence of Ca^{2+} ions, but only when a Ca^{2+} concentration higher than a critical concentration was used. Nano-domains dimensions of AFG produced using a $CaCl_2$/ALG ratio lower than the CRMF were in accordance with the values obtained by Badita et al. (Badita, et al., 2016). In addition, He et al. (He, et al., 2016) reported the formation of "nuclei" of gelation when $CaCl_2$/ALG ratio lower than a critical value was used. When a $CaCl_2$/ALG ratio lower than the CRMF was used for the production of AFG, some cross-linking points were generated; however, it appears that the Ca^{2+} concentration was not enough to crosslink all the α-L-guluronate (G) monomers of ALG that are responsible for the formation of the egg-box model (Braccini & Pérez, 2001). The non-crosslinked residues of polymer chains were able to interact with other non-crosslinked chains, explaining the formation of an extended network all over the whole material. Samples produced with a $CaCl_2$/ALG ratio higher than the CRMF were able to fully form microparticles. The folding of ALG polymer chains on themselves is a process induced by the applied shear regime. Ca^{2+} ions can "lock" ALG chains in position only when a concentration high enough to achieve a full crosslinking is used. After the removal of the shear regime, due to the full crosslinking of ALG, polymer chains were unable to unfold and interact with other ALG chains, but stable microparticles could still be formed. Even when a $CaCl_2$/ALG ratio lower than the CRMF was used, ALG folded on themselves, but due to the lack of a complete crosslinking, they were able to unfold and interact with each other, obtain an extended matrix, after the removal of the shear regime. In that case, only "pre-particles" within an ALG matrix could be identified by PSD analyses. However, due to their small dimensions they could not be visualised using the optical microscope.

3.1.2 Release behaviour

Nicotinamide loaded alginate fluid gels NFG-025 and NFG-035 were produced respectively using a $CaCl_2$/ALG ratio lower (0.25% $CaCl_2$ concentration) and higher (0.35% $CaCl_2$ concentration) than the CRMF; they were produced in the presence of NIC (0.10% w/w),

as described in the section 2.2.2 (Nicotinamide fluid gels). These two formulations were chosen with a view to understand how the release behaviour of the incorporated active compound is affected by the formed particle sizes. NIC was chosen as a model active because of its small dimension and its low molecular weight (122.13 g/mol) to avoid its physical entrapment into the gel-network, which would limit the diffusion into the release medium. Additionally, NIC is a highly hydrophilic molecule and displays a very high water solubility (>500 mg/mL at 25 °C), which is a suitable characteristic for the production of water-based fluid gels (Budavari, 1996). Additionally, the release profiles of these materials were compared to that of a NIC water solution and a NIC and ALG (2% w/w) water solution, both containing 0.10% w/w of the active (National Center for Biotechnology Information. PubChem Database. Nicotinamide), in order to fully understand if and how the $CaCl_2$ presence affects release behaviour (Figure 2).

As depicted from Figure 2, the formation of microparticles did not prevent the diffusion of NIC out of AFG. In fact, NFG-025 and NFG-035 presented the same release profile. Comparing these two curves with the one of NIC water solution, it can be observed that both AFG formulations were able to slightly slow down the release of NIC. This delay is obvious even when comparing the NIC&ALG solution curve with the NIC water solution one; however, the delay effect is enhanced in the presence of $CaCl_2$. It is possible to conclude that AFG are able to slow down the diffusion of the loaded NIC and this effect is due to a combination of the ALG and $CaCl_2$ presence. The delay ability can be attributed to the increase of viscosity of the solutions as suggested by Secouard et al. (Secouard, et al., 2003), in a release experiments of limonene from three different polysaccharide based water solutions and gel systems. They suggested that materials viscosities contribute significantly in limonene retention with the formulation and on its release behaviour.

3.2 Freeze drying

Freeze drying experiments were carried out to investigate the effect of processing time and $CaCl_2$ concentration, used during material production step, on samples moisture content and water activity. Rheological properties and particle size distributions were studied on both non freeze-dried (AFG) and freeze-dried and rehydrated (FD-AFG) fluid gels

300 formulations. ALG concentration was fixed at 2% w/w and three different fluid gels were
301 prepared using $CaCl_2$ concentration of 0.15%, 0.25% and 0.35.

302

303 3.2.1 Moisture content and water activity

304 Normalised moisture content (NMC) and water activity (a_w) were measured for 48 h
305 at different time intervals during the freeze drying experiments. The values obtained
306 alongside the corresponding standard deviations are shown in Figure 3.

307 From Figure 3a, it is possible to observe that the first stage of drying (about 18 h) was
308 quite fast and characterised by a constant rate. Specifically, for AFG at this stage sublimation
309 of the ice formed from inter-particle water took place, with a drying rate of about 0.02 h^{-1},
310 whereas for the alginate solution the process was faster (approx. 0.05 h^{-1}), likely due to the
311 absence of aggregates that act as a resistance to heat and mass transfer. As a result, AFG at
312 18h drying still showed a NMC around 0.4, while the solution was already dried. Thereafter,
313 for fluid gels a falling rate was observed up to 30 h, related to the intra-particle ice
314 sublimation. After 30 h, a zero drying rate with no substantial changes to moisture content
315 was recorded, i.e. all free water was removed from the samples. The experimental values
316 measured for a_w of the materials during drying, reported in Figure 3b, showed a slightly
317 different behaviour in the first stage. In fact, water activity remained nearly unchanged for 6h
318 in the case of the alginate solution and 18 h in the case of AFG and then gradually decreased
319 until achieving a constant value at 48 h. From these diagrams, it can be concluded that at least
320 48 h drying is needed for AFG to lower both a_w and NMC under the threshold limits (0.6 and
321 0.1, respectively (Brown, et al., 2010; de Bruijn, et al., 2016)) and, therefore, prevent microbial
322 growth.

323 The effect of fluid gel formation on alginate drying behaviour can be appreciated in
324 the first hours of drying (until 18 hours). In fact, for the sample not formed by a fluid gel (no
325 $CaCl_2$ added), the NMC decreased more rapidly if compared to materials in which some
326 amount of $CaCl_2$ was used. A similar trend can be identified from the water activity (a_w) curves;
327 especially at 18 hours of drying time big differences between samples can be seen. The slower
328 drying kinetics of AFG, when compared to an ALG solution in which no $CaCl_2$ was added, can
329 be due to the formation of a gel network in which water is entrapped between alginate
330 polymer chains leading to more time being required to remove water from that network.

Additionally, comparing the a_w and NMC curves obtained at different $CaCl_2$ concentrations for AFG samples (Figure 3a and 3b), it can be seen that there is negligible difference among them, suggesting that once the network is formed, this parameter does not have substantial effect on the gel drying.

3.2.2 Rehydration performance

FD samples were rehydrated, following the procedure reported in section 2.9, to assess the impact of the freezing/drying on the material properties of fluid gels. Rehydration is one of the key parameters that quantify the quality of a dried product as it describes its ability to reacquire the initial amount of water within its structure. Rehydration is a complex phenomenon, in which different mechanisms take place: water absorption into the dried product, diffusion through the porous network and swelling of the structure (Lopez-Quiroga, et al., 2019; Maldonado, et al., 2010; Ratti, 2008). Rehydrated samples were characterised in terms of viscosity, PSD and release behaviour and compared with unprocessed (non-freeze dried) fluid gels.

3.2.3 Recovery of rheological properties

The rheological behaviour of rehydrated fluid gel samples having different $CaCl_2$ content was compared to that of systems prior to FD. Samples were rehydrated for 1 hour before recording viscosity measurements. Viscosity curves for the different formulations are presented in Figure 4.

It is possible to notice that for AFG_2%_0.15% and AFG_2%_0.25%, viscosity curves before FD and after FD/rehydration are almost overlapping. It can be stated that freeze-dried materials with a $CaCl_2$ concentration of 0.15% or 0.25% were able to fully recover the rheological behaviour they had before freeze-drying. AFG_2%_0.15% and AFG_2%_0.25% were produced using a 2% ALG concentration and, as shown in Figure 4, they were not able to produce microparticles. The comparison between the viscosity curves of AFG_2%_0.35% in the fresh and dried/rehydrated form showed more significant changes (Figure 6c). More specifically, an overall decrease in the shear viscosity can be observed and, in particular, the difference with the untreated material becomes more evident as shear rate increases. This behaviour can be due to the inability of AFG_2%_0.35% to fully reabsorb the added water or

by its delay in doing that. Additional rehydration experiments were carried out on freeze-dried AFG_2%_0.35%, increasing the rehydration time up to 48h, to assess if they were able to recover the rheological properties they had before freeze drying by prolonging the time of the rehydration step; however, the viscosity profile was not restored even after 2 days of rehydration in the shaker incubator. This behaviour suggests that AFG produced using a $CaCl_2$/ALG ratio higher than the CRPF, i.e. when microparticles formation is achieved, cannot recover the rheological properties they had before FD. This set of experiments showed that the rehydration of AFG, and the complete recovery of the rheological properties they had before the FD, is achievable only when materials were prepared using a $CaCl_2$/ALG ratio lower than CRPF. Below that ratio, polymer chains are not fully cross-linked leaving some empty zones between them in the alginate gel formed. Because of the presence of less cross-linking junctions, polymer chains present a higher mobility than polymer chains of fully cross-linked materials (when a $CaCl_2$/ALG ratio higher than the CRMF was used). The rehydrated AFG_2%_0.35% samples were not visually homogeneous and regions having higher particle concentration and regions at higher water concentration could be identified. This higher mobility may explain why viscosity profiles before and after FD completely match solely for samples not completely cross-linked. In fact, the more mobile polymer chains are less rigid and they can move more and faster to fit the water molecules between them. In contrast, polymer chains having a lower mobility due to the presence of more cross-linking points, take more time to fit all water molecules or just a fraction of the removed water molecules can be reabsorbed.

In order to identify the time needed for AFG produced using a $CaCl_2$/ALG ratio lower than the CRMF to recover the viscosity they had before FD, an additional rehydration experiment was carried out on AFG_2%_0.25% using a rehydration time of 5 min and 10 min in the shacking incubator before performing the rheological test. A comparison among the resulting viscosity curves is reported in Figure 5.

From Figure 5 becomes evident that the complete recovery of viscosity was achieved after approximately 10 min of rehydration time. It can be concluded that AFG produced using a $CaCl_2$/ALG ratio lower than the CRMF are able to fully recover the rheological properties they had before FD in a short time.

3.2.3 Particle Size distribution

The PSD of rehydrated samples of AFG_2%_0.15%, AFG_2%_0.25% and AFG_2%_0.35% were compared to those of the samples before FD to identify if some particle aggregation was induced by the drying process. Samples were rehydrated for 1 hour before performing particle size measurements using the Mastersizer as described in section 2.4.1. PSD curves are displayed in Figure 6.

The PSD curves after rehydration were perfectly overlapping with the curves obtained from materials before FD. It is possible to conclude that AFG do not form aggregates during the freeze-drying process and that they can retain their initial sizes.

3.2.4 Release behaviour of nicotinamide-loaded fluid gels

After NFG production, a fraction of both NFG_025 and NFG-035 was freeze-dried, as described in section 2.6 (Freeze drying), until constant weight (48 h). Freeze dried samples were then rehydrated for 1 hour and release of the active over time was studied, as described in section 2.10 (In vitro release), to highlight the influence of FD on the release behaviour of NIC. The NIC release profiles from FG before drying and following drying and rehydration are depicted in Figure 7 for two different concentrations of the active:

As can be seen in Figure 7a-b, both FD and rehydration processes do not seem to affect the release behaviour of NIC from AFG; in fact, release curves are almost overlapping. In order to better understand the release behaviour of NIC a model fitting analysis was conducted: data obtained from in vitro release studies of NFG formulations were used to fit a mathematical model as described in section 2.11 Data fitting and the obtained parameters are reported in Table 3:

As described by Rinaki et al. (Rinaki, et al., 2003), the *n* parameter obtained from data fitting of eq. 2 describes the mechanism of drug release. As can be noticed from Table 3, this value is almost constant for all in vitro experiments and it is in the range between 0.51-0.59. As reported by the same authors and by Korsmeyer et al. (Korsmeyer, et al., 1983; Rinaki, et al., 2003), n values in the range 0.4-0.65 are related to pure diffusion mechanism (anomalous non-Fickian diffusion) of drug. In NFG the release of NIC can be related to its diffusion through the ALG matrix; this is very similar to the diffusion of NIC from a water solution or from a water and alginate solution. This supports the theory that no drug-matrices interactions were

formed between NIC and AFG. In a previous reported study, the interaction between tryptophan and AFG were recorded (Smaniotto, et al., 2019). However, in that case the amount of drug detected during in vitro release studies was not equal to the overall amount of drug introduced in AFG and the amount released was also affected by storage time, suggesting a possible interaction between tryptophan and alginate polymer chains, as reported in literature by Yang et al. (Yang, et al., 2015). As described by Korsmeyer et al. (Korsmeyer, et al., 1983), the kinetic constant *k* is characteristic of each drug-matrix system. As can be seen in Table 3, *k* values of NFG-0.35 are substantially different between the "untreated" material and the one after the drying and rehydration processes. As reported above (see section 3.2.2 Recovery of rheological properties), AFG made using a $CaCl_2$/ALG ratio higher than the CRMF, as in the case of NFG-0.35, were not able to be completely rehydrated and their rheological properties were affected by the drying and rehydration steps. Changes in *k* values of NFG-0.35 confirm that AFG made using a $CaCl_2$/ALG ratio higher than the CRMF cannot be completely rehydrated. This is not true for AFG made using a $CaCl_2$/ALG ratio lower than the CRMF, as the *k* values of NFG-0.25 is very similar to the one of the same sample submitted to freeze drying and rehydration processes, confirming that a complete rehydration of the matrix can be achieved, as showed in section 3.2.2 Recovery of rheological properties.

It is possible to conclude that AFG are able to slow down the diffusion of the loaded NIC even after FD. Additionally, freeze drying is a suitable technique for preserving AFG by decreasing their moisture content and, consequently, their water activity, preventing the bacterial growth. Rehydration can restore the release behaviour they had before freeze drying.

4. Conclusions

In this work, the suitability of freeze drying as preservation method for alginate fluid gels was investigated. The effect of particle dimensions on drying kinetics and rehydration behaviour of these materials was studied. It was demonstrated that the drying and rehydration processes do not affect the particle size distribution. However, the rheological properties of AFG can be completely recovered only when materials where made using a $CaCl_2$/ALG ratio that allowed the formation of nanoparticles. Preliminary encapsulation experiments of NIC in AFG were also carried out, showing that the release behaviour of this active from AFG was

not modified by the drying/rehydration processes when AFG were composed of nanoparticles. This showed to be the most suitable system to deliver the active compound. On the other hand, data fitting models of in vitro release experiments showed some changes in the release behaviour of NIC after freeze drying and rehydration of AFG made of microparticles. This is probably due to the fact that microparticles-based AFG cannot be fully rehydrated. More experiments should be conducted in the future, loading other types of actives in AFG to investigate their usage as materials for the controlled release overtime of actives. These results can be relevant from both a scientific and industrial point of view, since they lead to a better understanding of the AFG behaviour and suggest that FD can be applied to extend their shelf life, without any compromise in the material properties.

Acknowledgement

This research was funded by the Engineering and Physical Sciences Research Council [grant number EP/K030957/1], the EPSRC Centre for Innovative Manufacturing in Food.

References

Badita, C. R., Aranghel, D., Radulescu, A., & Anitas, E. M. (2016). The study of the structural properties of very low viscosity sodium alginate by small-angle neutron scattering. *AIP Conference Proceedings, 1722*(1), 220007.

Barbosa, J., Borges, S., Amorim, M., Pereira, M. J., Oliveira, A., Pintado, M. E., & Teixeira, P. (2015). Comparison of spray drying, freeze drying and convective hot air drying for the production of a probiotic orange powder. *Journal of Functional Foods, 17*, 340-351.

Bonifacio, M. A., Gentile, P., Ferreira, A. M., Cometa, S., & De Giglio, E. (2017). Insight into halloysite nanotubes-loaded gellan gum hydrogels for soft tissue engineering applications. *Carbohydrate Polymers, 163*, 280-291.

Braccini, I., & Pérez, S. (2001). Molecular Basis of Ca2+-Induced Gelation in Alginates and Pectins: The Egg-Box Model Revisited. *Biomacromolecules, 2*(4), 1089-1096.

Brown, Z. K., Fryer, P. J., Norton, I. T., Bakalis, S., & Bridson, R. H. (2008). Drying of foods using supercritical carbon dioxide — Investigations with carrot. *Innovative Food Science & Emerging Technologies, 9*(3), 280-289.

Brown, Z. K., Fryer, P. J., Norton, I. T., & Bridson, R. H. (2010). Drying of agar gels using supercritical carbon dioxide. *The Journal of Supercritical Fluids, 54*(1), 89-95.

Budavari, S. (1996). *The Merck Index - An Encyclopedia of Chemicals, Drugs, and Biologicals.* Whitehouse Station, NJ.: Merck and Co.

Cardea, S., Pisanti, P., & Reverchon, E. (2010). Generation of chitosan nanoporous structures for tissue engineering applications using a supercritical fluid assisted process. *Journal of Supercritical Fluids, 54*(3), 290-295.

Cassanelli, M., Prosapio, V., Norton, I., & Mills, T. (2018). Acidified/basified gellan gum gels: The role of the structure in drying/rehydration mechanisms. *Food Hydrocolloids, 82*, 346-354.

Cassanelli, M., Prosapio, V., Norton, I., & Mills, T. (2019). Role of the Drying Technique on the Low-Acyl Gellan Gum Gel Structure: Molecular and Macroscopic Investigations. *Food and Bioprocess Technology, 12*(2), 313-324.

Chung, C., Degner, B., & McClements, D. J. (2014). Development of Reduced-calorie foods: Microparticulated whey proteins as fat mimetics in semi-solid food emulsions. *Food Research International, 56*, 136-145.

de Bruijn, J., Rivas, F., Rodriguez, Y., Loyola, C., Flores, A., Melin, P., & Borquez, R. (2016). Effect of vacuum microwave drying on the quality and storage stability of strawberries. *Journal of Food Processing and Preservation, 40*, 1104-1115.

De Marco, I., & Reverchon, E. (2017). Starch aerogel loaded with poorly water-soluble vitamins through supercritical CO2 adsorption. *Chemical Engineering Research and Design, 119*, 221-230.

Fernández Farrés, I., Douaire, M., & Norton, I. T. (2013). Rheology and tribological properties of Ca-alginate fluid gels produced by diffusion-controlled method. *Food Hydrocolloids, 32*(1), 115-122.

Fernández Farrés, I., Moakes, R. J. A., & Norton, I. T. (2014). Designing biopolymer fluid gels: A microstructural approach. *Food Hydrocolloids, 42*, 362-372.

Franco, P., Aliakbarian, B., Perego, P., Reverchon, E., & De Marco, I. (2018). Supercritical Adsorption of Quercetin on Aerogels for Active Packaging Applications. *Industrial & Engineering Chemistry Research, 57*(44), 15105-15113.

García, Alfaro, M. C., Calero, N., & Muñoz, J. (2014). Influence of polysaccharides on the rheology and stabilization of α-pinene emulsions. *Carbohydrate polymers, 105*, 177-183.

García, Trujillo, L. A., Muñoz, J., & Alfaro, M. C. (2018a). Gellan gum fluid gels: influence of the nature and concentration of gel-promoting ions on rheological properties. *Colloid and Polymer Science, 296*(11), 1741-1748.

García, Trujillo, L. A., Muñoz, J., & Alfaro, M. C. (2018b). Gellan gum fluid gels: influence of the nature and concentration of gel-promoting ions on rheological properties. *Colloid and Polymer Science*.

Garrec, D. A., & Norton, I. T. (2012). Understanding fluid gel formation and properties. *Journal of food engineering, 112*(3), 175-182.

He, X., Liu, Y., Li, H., & Li, H. (2016). Single-stranded structure of alginate and its conformation evolvement after an interaction with calcium ions as revealed by electron microscopy. *RSC Advances, 6*(115), 114779-114782.

Hu, Y., Que, T., Fang, Z., Liu, W., Chen, S., Liu, D., & Ye, X. (2013). Effect of Different Drying Methods on the Protein and Product Quality of Hairtail Fish Meat Gel. *Drying Technology, 31*(13-14), 1707-1714.

Jin, H., Nishiyama, Y., Wada, M., & Kuga, S. (2004). Nanofibrillar cellulose aerogels. *Colloids and Surfaces A: Physicochemical and Engineering Aspects, 240*(1-3), 63-67.

Karam, M. C., Petit, J., Zimmer, D., Baudelaire Djantou, E., & Scher, J. (2016). Effects of drying and grinding in production of fruit and vegetable powders: a review. *Journal of food engineering, 188*, 32-49.

Korsmeyer, R. W., Gurny, R., Doelker, E., Buri, P., & Peppas, N. A. (1983). Mechanisms of solute release from porous hydrophilic polymers. *International Journal of Pharmaceutics, 15*(1), 25-35.

Le Révérend, B. J. D., Norton, I. T., Cox, P. W., & Spyropoulos, F. (2010). Colloidal aspects of eating. *Current Opinion in Colloid & Interface Science, 15*(1), 84-89.

Long, L. Y., Weng, Y. X., & Wang, Y. Z. (2018). Cellulose aerogels: Synthesis, applications, and prospects. *Polymers, 8*(6).

Lopez-Quiroga, E., Prosapio, V., Fryer, P. J., Norton, I. T., & Bakalis, S. (2019). Model discrimination for drying and rehydration kinetics of freeze-dried tomatoes. *Journal of Food Process Engineering*, e13192.

Mahdi, M. H., Conway, B. R., Mills, T., & Smith, A. M. (2016). Gellan gum fluid gels for topical administration of diclofenac. *International Journal of Pharmaceutics, 515*(1), 535-542.

Maldonado, S., Arnau, E., & Bertuzzi, M. (2010). Effect of temperature and pretreatment on water diffusion during rehydration of dehydrated mangoes. *Journal of food engineering, 96*(3), 333-341.

Mao, B., Divoux, T., & Snabre, P. (2017). Impact of saccharides on the drying kinetics of agarose gels measured by in-situ interferometry. *Scientific Reports, 7*, 41185.

McHugh, D. J. J. P., & Pap, U. o. P. f. C. S. F. F. T. (1987). Production, properties and uses of alginates. *288*, 58-115.

National Center for Biotechnology Information. PubChem Database. Nicotinamide, C., https://pubchem.ncbi.nlm.nih.gov/compound/936 (accessed on Apr. 27, 2019).

Norton, Frith, W. J., & Ablett, S. (2006). Fluid gels, mixed fluid gels and satiety. *Food Hydrocolloids, 20*(2), 229-239.

Norton, Gonzalez Espinosa, Y., Watson, R. L., Spyropoulos, F., & Norton, I. T. (2015). Functional food microstructures for macronutrient release and delivery. *Food & Function, 6*(3), 663-678.

Norton, Jarvis, D. A., & Foster, T. J. (1999). A molecular model for the formation and properties of fluid gels. *International Journal of Biological Macromolecules, 26*(4), 255-261.

Prosapio, V., & Norton, I. (2017a). Influence of osmotic dehydration pre-treatment on oven drying and freeze drying performance. *LWT - Food Science and Technology, 80*, 401-408.

Prosapio, V., & Norton, I. (2018). Simultaneous application of ultrasounds and firming agents to improve the quality properties of osmotic + freeze-dried foods. *LWT, 96*, 402-410.

Prosapio, V., Norton, I., & De Marco, I. (2017b). Optimization of freeze-drying using a Life Cycle Assessment approach: Strawberries' case study. *Journal of Cleaner Production, 168*, 1171-1179.

Ratti, C. (2001). Hot air and freeze-drying of high-value foods: a review. *Journal of food engineering, 49*, 311-319.

Ratti, C. (2008). *Advances in food dehydration*: CRC Press.

Rinaki, E., Valsami, G., & Macheras, P. (2003). The power law can describe the 'entire' drug release curve from HPMC-based matrix tablets: a hypothesis. *International Journal of Pharmaceutics, 255*(1), 199-207.

Sanchez, V., Baeza, R., Galmarini, M. V., Zamora, M. C., & Chirife, J. (2013). Freeze-Drying Encapsulation of Red Wine Polyphenols in an Amorphous Matrix of Maltodextrin. *Food and Bioprocess Technology, 6*(5), 1350-1354.

Secouard, S., Malhiac, C., Grisel, M., & Decroix, B. (2003). Release of limonene from polysaccharide matrices: viscosity and synergy effect. *Food Chemistry, 82*(2), 227-234.

Siepmann, J., Streubel, A., & Peppas, N. A. (2002). Understanding and Predicting Drug Delivery from Hydrophilic Matrix Tablets Using the "Sequential Layer" Model. *Pharmaceutical Research, 19*(3), 306-314.

Smaniotto, F., Zafeiri, I., Prosapio, V., & Spyropoulos, F. (2019). *Use of Alginate Fluid Gel Microparticles to Modulate the Release of Hydrophobic Actives*.

Smirnova, I., Mamic, J., & Arlt, W. (2003). Adsorption of Drugs on Silica Aerogels. *Langmuir, 19*(20), 8521-8525.

Stevenson, A., Cray, J. A., Williams, J. P., Santos, R., Sahay, R., Neuenkirchen, N., McClure, C. D., Grant, I. R., Houghton, J. D. R., Quinn, J. P., Timson, D. J., Patil, S. V., Singhal, R. S., Antón, J., Dijksterhuis, J., Hocking, A. D., Lievens, B., Rangel, D. E. N., Voytek, M. A., Gunde-Cimerman, N., Oren, A., Timmis, K. N., McGenity, T. J., & Hallsworth, J. E. (2015). Is there a common water-activity limit for the three domains of life? *The ISME Journal, 9*, 1333-1351.

Tiwari, S., Chakkaravarthi, A., & Bhattacharya, S. (2015). Imaging and image analysis of freeze-dried cellular solids of gellan and agar gels. *Journal of food engineering, 165*, 60-65.

Torres, O., Murray, B., & Sarkar, A. (2016). Emulsion microgel particles: Novel encapsulation strategy for lipophilic molecules. *Trends in Food Science & Technology, 55*, 98-108.

Vega-Gálvez, A., Zura-Bravo, L., Lemus-Mondaca, R., Martinez-Monzó, J., Quispe-Fuentes, I., Puente, L., & Di Scala, K. (2015). Influence of drying temperature on dietary fibre, rehydration properties, texture and microstructure of cape gooseberry (physalis peruviana l.). *Journal of Food Science and Technology, 52*, 2304-2311.

Wang, Y., Chang, Y., Xue, Y., Li, Z., Wang, Y., & Xue, C. (2016). Rheology and microstructure of heat-induced fluid gels from Antarctic krill (Euphausia superba) protein: Effect of pH. *Food Hydrocolloids, 52*, 510-519.

Yang, Y., Qian, J., & Ming, D. (2015). Docking polysaccharide to proteins that have a Tryptophan box in the binding pocket. *Carbohydrate Research, 414*, 78-84.

613

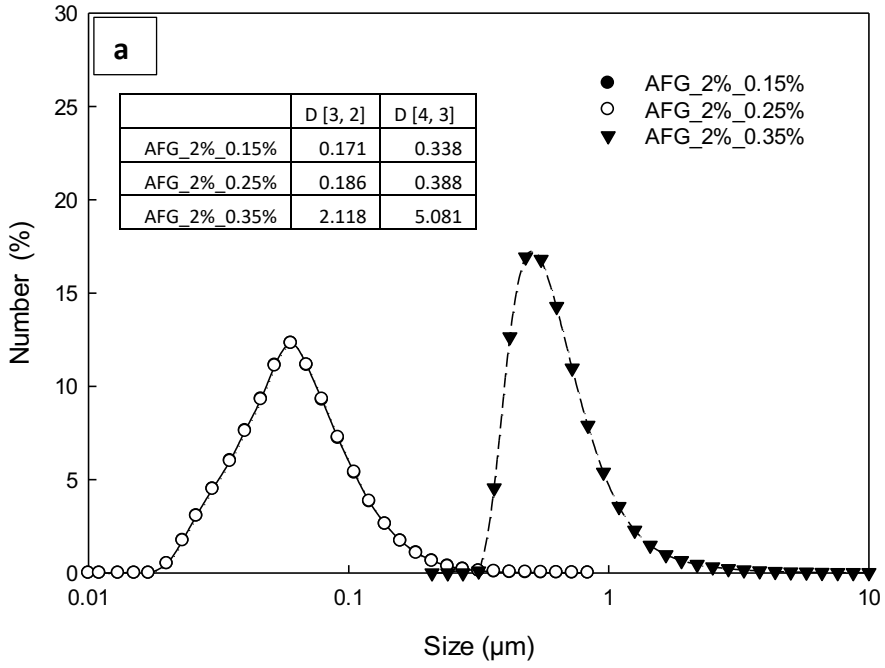

	D [3, 2]	D [4, 3]
AFG_2%_0.15%	0.171	0.338
AFG_2%_0.25%	0.186	0.388
AFG_2%_0.35%	2.118	5.081

614

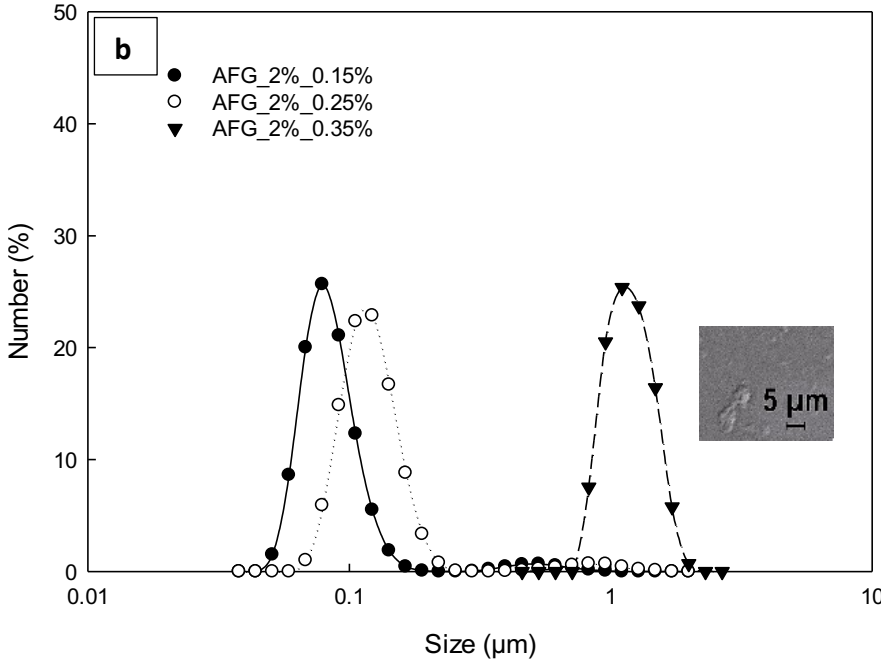

615

616 *Figure 1- PSD curves of AFG produced by using 2% ALG (w/w): (a) Mastersizer, (b) Zetasizer.*

617

618

619

620

621

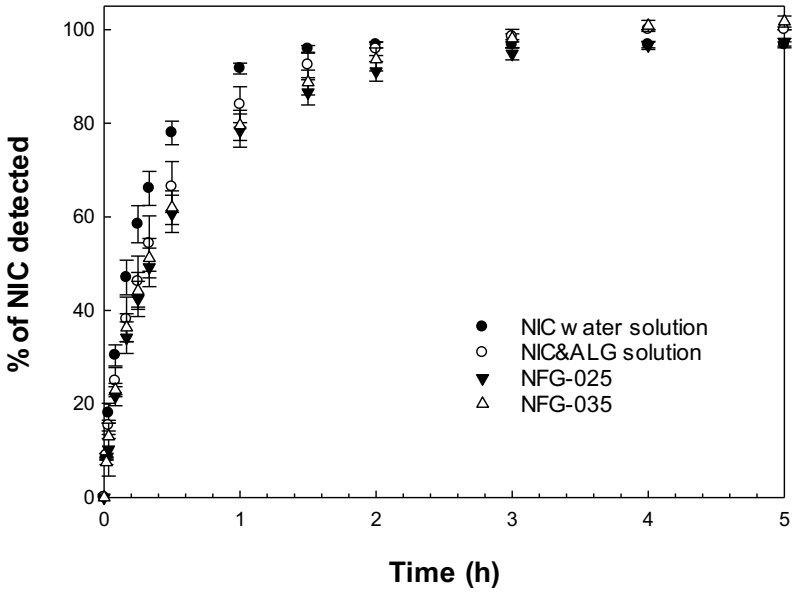

622

623 Figure 2- In vitro release profile of nicotinamide (National Center for Biotechnology Information. PubChem
624 Database. Nicotinamide) from NIC in aqueous medium, NIC&ALG solution, and NIC-loaded alginate fluid gels
625 produced using different concentrations of $CaCl_2$ (NFG-025 and NFG-035).

626

627

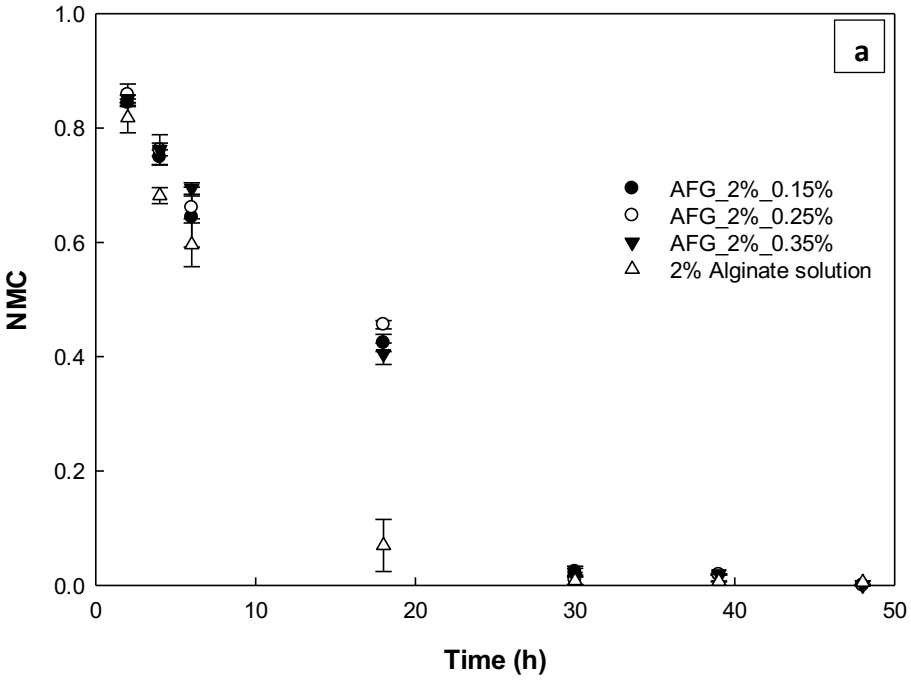

628

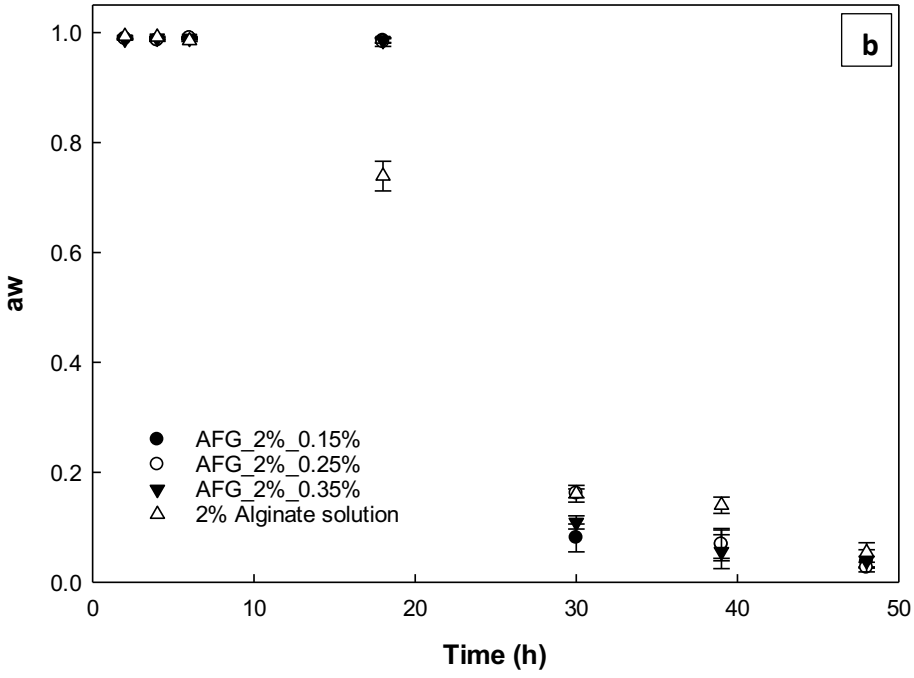

629

630 *Figure 3- Drying kinetics of fluid gels at 2% ALG (w/w) and different $CaCl_2$ concentrations: (a) Normalised*
631 *Moisture Content; (b) water activity.*

632

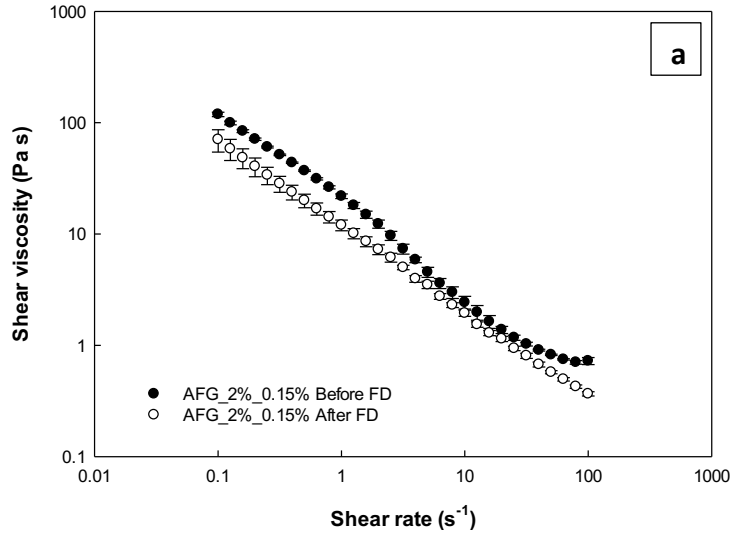

633

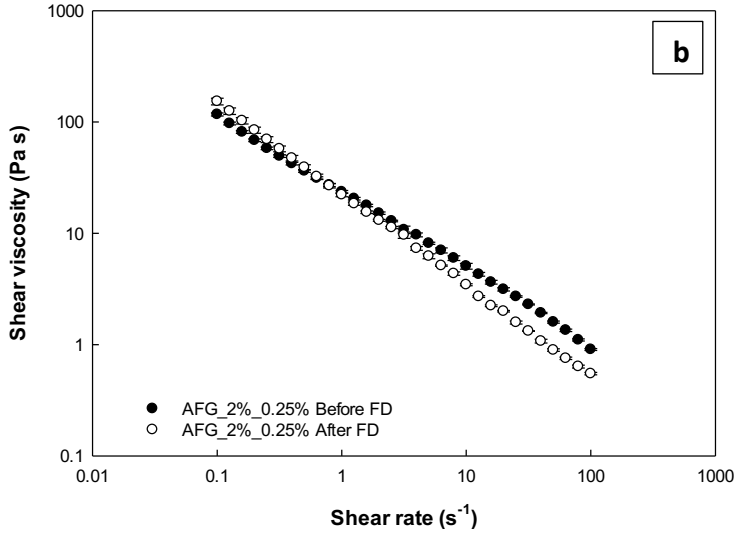

634

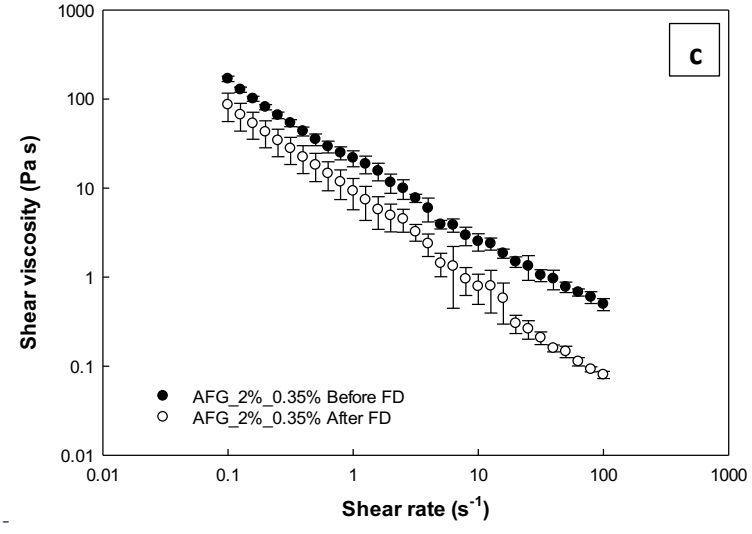

635

636 *Figure 4: Shear viscosity curves of blank AFG before freeze drying and after drying/rehydration: (a) 0.15% $CaCl_2$;*
637 *(b) 0.25% $CaCl_2$; (c) 0.35% $CaCl_2$.*

638

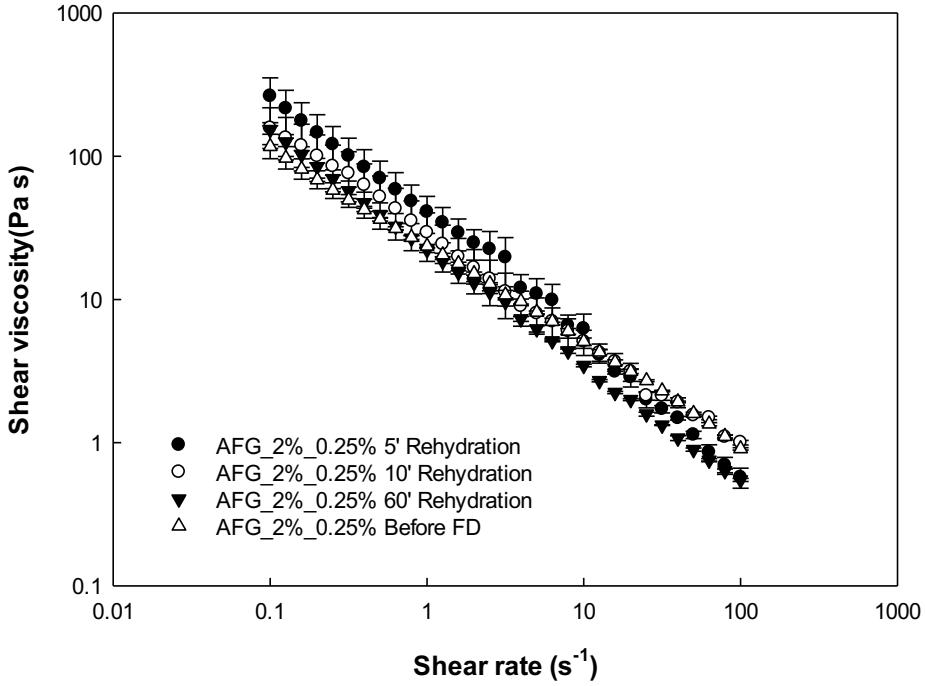

Figure 5- Shear viscosity curves of AFG-025 as a function of the rehydration time

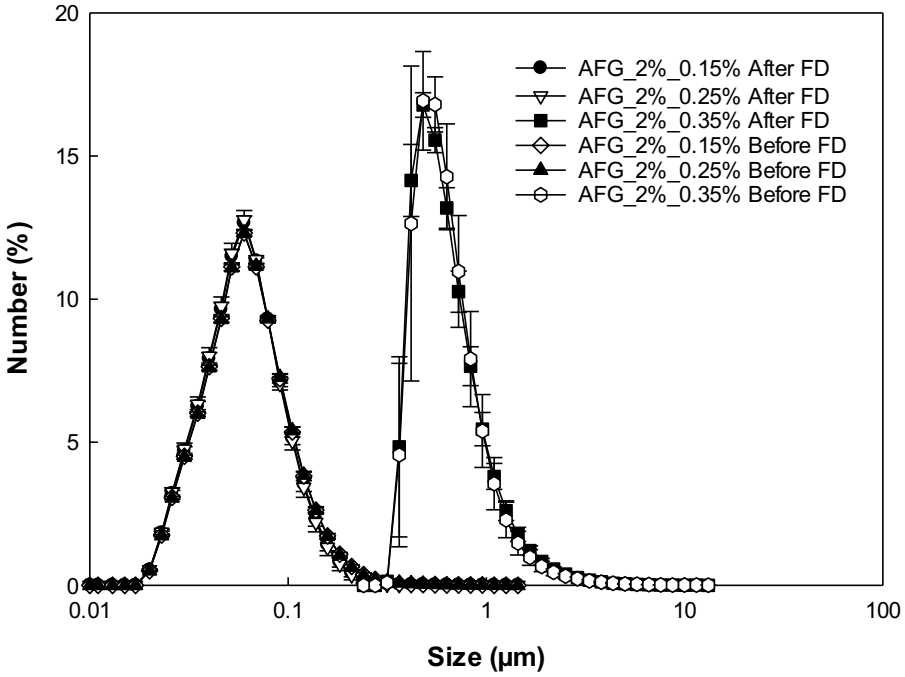

Figure 6- PSD curves of blank (no active) AFG before freeze drying and after drying and rehydration

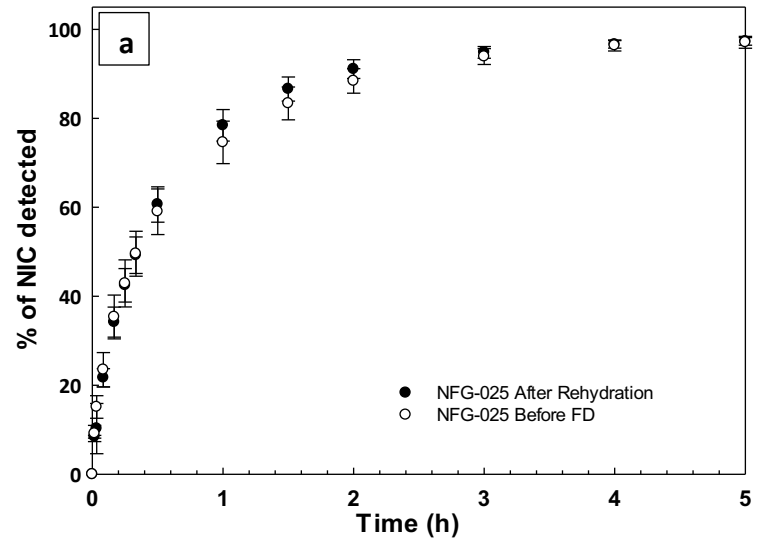

647

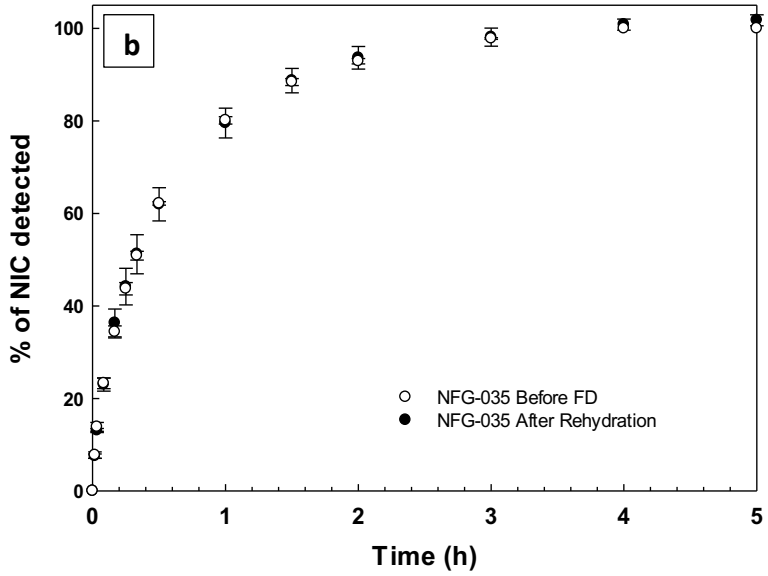

648

649 Figure 7- In vitro release profiles of NIC from forming nanoparticles AFG (a) and forming microparticles AFG (b)
650 before freeze drying and after drying and rehydration.

651

652

Table 1-ALG and $CaCl_2$ concentrations used for sample preparations

Sample	Alginate concentration (w/w)	$CaCl_2$ concentration (w/w)
AFG_2%_0.15%	2%	0.15%
AFG_2%_0.25%	2%	0.25%
AFG_2%_0.35%	2%	0.35%

Table 2- ALG and $CaCl_2$ concentrations used for sample preparations

Sample	Alginate concentration (w/w)	$CaCl_2$ concentration (w/w)
AFG_1%_0.15%	1%	0.15%
AFG_1%_0.25%	1%	0.25%
AFG_3%_0.35%	3%	0.35%
AFG_3%_0.45%	3%	0.45%

Table 3 – k, n, R^2, parameters obtained from eq. 2 data fitting

	NFG-0.25	NFG-025 after rehydration	NFG-0.35	NFG-0.35 after rehydration	NIC Solution	NIC&ALG
k	0.9526 (± 0.0835)	0.8835 (± 0.0518)	0.9187 (± 0.0785)	0.3911 (± 0.0504)	1.3440 (± 0.1925)	0.9814 (± 0.0488)
n	0.5826 (± 0.0654)	0.5118 (± 0.0413)	0.5578 (± 0.0625)	0.5600 (± 0.0396)	0.5851 (± 0.0887)	0.5464 (± 0.0361)
R^2	0.995	0.997	0.995	0.998	0.994	0.998